benzene to yield 288 mg (60%) of **13b**: mp 165-166 °C dec; IR (KBr) 2100, 1690 cm^{-1}; ^1H NMR ($CDCl_3$) δ 6.9-83 (m, 9 H).

(b) (3-Azidobenzoyl)imidazole (10b): 56%; mp 81-83 °C (benzene-hexane); IR ($CHCl_3$) 2100, 1690 cm^{-1}; ^1H NMR ($CDCl_3$-acetone-d_6) δ 7.12-8.0 (m, 7 H).

(c) (4-Azidobenzoyl)imidazole (12b): 70%; mp 66-68 °C (benzene-hexane); IR ($CHCl_3$) 2100, 1685 cm^{-1}; ^1H NMR ($CDCl_3$) δ 7.0-8.1 (m, 7 H).

(d) (3-Azido-5-nitrobenzoyl)imidazole (13b): 18%; mp 100-103 °C (benzene-hexane); IR (KBr) 2120, 1705, 1530, 1520, 1380, 1350, 1265, 960 cm^{-1}; ^1H NMR ($CDCl_3$) δ 8.5 (s, 1 (H), 8.0 (s, 1 H), 7.2 (s, 2 H), 6.9 (s, 1 H).

EPR Experiments. Solutions of methyl esters **10c-13c** (1×10^{-3} M) in cyclohexane, toluene, 2-propanol, methanol, and glycerol-water (1:1, pH 3.0) were prepared. The solutions (0.5 mL) were placed in quartz EPR tubes, degassed by 3 freeze-jump-thaw cycles, and then sealed under vacuum. Samples of modified enzymes **10a-13a** were prepared by putting 12.5 mg of **10a-13a** in quartz EPR tubes and adding 0.5 mL of glycerol-water (1:1, pH 3.0), which was previously deoxygenated by bubbling with nitrogen gas. The solutions obtained were frozen in liquid nitrogen and sealed under vacuum.

A Varian E-line Series 112 spectrometer was used to obtain EPR spectra. To obtain spectra at 77 K, the samples were immersed in a quartz Dewar (Wilmad) containing liquid nitrogen, which fit into the cavity of the EPR spectrometer. EPR spectra were obtained at 173-174 K by using the Varian variable-temperature controller.

The output of a 1000-W mercury-xenon arc lamp passing through a $CuSO_4$ solution filter ($\lambda > 320$ nm) was focused into the cavity for photolysis. The samples were photolyzed for 30 s, and the field positions of the triplet nitrene signals were recorded. The kinetics of the decay reaction of the triplet nitrene at 173-174 K were measured by observing the decrease in the intensity of the signals at regular intervals. Pseudo-first-order rate constants were obtained by fitting the initial 20% of the signal decay.[23]

Product Studies of Methyl *m*-Azidobenzoate (10c) in Toluene. Solutions of **10c** in toluene for product studies (0.5 mL) were sealed in 5-mm Pyrex tubes, which were prewashed with ammonium hydroxide solution and oven-dried. The samples were degassed by using 3 freeze-jump-thaw cycles, sealed under vacuum, and photolyzed for 4 h with two southern New England ultraviolet RPR 3500-Å lamps. The product mixtures were analyzed with a Hewlett-Packard 8530 A gas chromatograph using a 6 ft × $^1/_8$ in. 5% SE-30 column. The yields and identities of the products were determined by coinjection of authentic samples and by mass spectroscopy.

Photochemistry of Modified Enzyme 10a. Samples were prepared by dissolving 93-94 mg each of native chymotrypsin and modified enzyme **10a** in 5 mL of aqueous HCl solution of pH 3.0. Solutions (1.0 mL) were placed in 6-mm Pyrex tubes previously cleaned and dried and sealed with rubber septa. The solutions were photolyzed for 2 h with four Southern New England ultraviolet RPR 3500-Å lamps.

The photolyzed enzyme solutions were treated with sufficient 25% aqueous hydrazine solution[24] to raise the pH of the solutions between pH 7 and 8. The samples were kept at that pH for 1 h to effect complete hydrolysis of the ester linkage in modified enzyme **10a**. The solutions were then passed through a column of Sephadex G-25 (10 cm × 1 cm) and eluted with aqueous HCl solution of pH 3.0. The eluent fractions with high absorbances at 280 nm were collected, and the enzyme was obtained by lyophilization using a Virtis Freeze Mobile 6 lyophilizer. In the control experiments, samples of native α-chymotrypsin and modified enzyme **10a** were photolyzed and treated with hydrazine and reisolated by lyophilization after being passed through a Sephadex G-25 column.

The enzymes, both photolyzed and unphotolyzed, were assayed using cinnamoyl imidazole at pH 5 as described in literature.[14]

General Procedure for the Preparation of Modified Enzymes 10a-13a. α-chymotrypsin (100 mg) was dissolved in 3.0 mL of 0.1 M acetate buffer (pH 5) in a centrifuge tube. To this was carefully added a solution of 10 mg of the acyl imidazole in 200 mL acetonitrile. After careful mixing for 15 minutes, the mixture was centrifuged to separate the solid material. The clear supernatant solution was immediately transferred onto a Sephadex G-25 column (40 cm × 2.5 cm) which was equilibrated with aqueous HCl solution (pH 3) and eluted with the same solution. Five-mL fractions were collected and monitored for the protein absorption at 280 nm. The fractions containing the protein were combined and lyophilized to obtain the modified enzyme.

Acknowledgment. We are indebted to Prof. Jakob Wirz and Fr. Gabrielle Persy for their help in obtaining the UV-vis spectrum of nitrene **14bT** and to the NSF U.S.-Switzerland international program for allowing M.S.P. to visit Basel, Switzerland. M.J.T.Y. is indebted to the Eastman Kodak Co. for a graduate fellowship, administered through the Organic Division of the American Chemical Society. Financial support of the NIH (Grant GM-24823-01A1) is gratefully acknowledged.

Observation of Secondary Bonding in Solution: Synthesis, NMR Studies, and the Crystal Structure of $Te^{VI}[OTe^{IV}(C_8H_8)(S_2P(OEt)_2)]_6$†

Dainis Dakternieks,*[1] Robert Di Giacomo,[2] Robert W. Gable,[2] and Bernard F. Hoskins*[2]

Contribution from the Department of Inorganic Chemistry, University of Melbourne, Parkville, Victoria 3052, Australia, and Division of Chemical and Physical Sciences, Deakin University, Waurn Ponds, Victoria 3217, Australia. *Received December 31, 1987*

Abstract: The compound $Te[OTe(C_8H_8)(S_2P(OEt)_2)]_6$ (**1**), an unexpected hydrolysis product of $C_8H_8Te[S_2P(OEt)_2]_2$, was subsequently synthesized under very mild conditions and appears to be the first organotellurium compound containing both tellurium(IV) and tellurium(VI). Crystals of **1** are triclinic, space group $P\bar{1}$: a = 14.287 (2), b = 14.579 (2), c = 14.652 (2) Å; α = 85.30 (1), β = 84.36 (1), γ = 60.20 (1)°; Z = 1. The central Te(VI) atom is surrounded octahedrally by six oxygen atoms, which bridge to Te(IV) centers. Each Te(IV) center is coordinated asymmetrically by a dithiophosphate ligand. The sulfur atom of the longer Te-S bond also forms a secondary interaction with an adjacent Te(IV) atom within the same molecule. Each Te(IV) atom has a stereochemically active lone electron pair occupying one of the coordination positions and results in a seven-coordinate 1:2:2:2 geometry. Variable-temperature ^{13}C, ^{31}P, and ^{125}Te NMR indicate that intramolecular monodentate-bidentate exchange of the dithiophosphate ligand is slow on the NMR time scale. NMR studies on $Te[OTe(C_8H_8)(S_2P(O^iPr)_2)]_6$ indicate that, as a result of extensive secondary bonding, this molecule is remarkably rigid in solution at room temperature, with the structure in solution being similar to that determined for $Te[OTe(C_8H_8)(S_2P(OEt)_2)]_6$ in the solid state. This represents the first occasion for which the secondary bonds observed in the solid state persist in solution.

Synthesis of known mixed-valent tellurium(IV)-tellurium(VI) complexes has until now involved use of the highly electron withdrawing ligand, $OTeF_5$.[3-6] The complex $Te(OTeF_5)_4$, characterized by ^{125}Te and ^{19}F NMR spectroscopies,[4] contains a central tellurium(IV) atom bonded via oxygen to four tellurium(VI) atoms. Complexes such as $F_4Te(OTeF_5)_2$, $F_2Te(OTeF_5)_4$, $FTe(OTeF_5)_5$, and $Te(OTeF_5)_6$, which contain Te(VI)-O-Te(VI) bonds, have also been studied.[3] The X-ray structure determi-

† Hexakis[[2-[(diethoxythiophosphoryl)thio]-1,3-dihydro-2λ⁴-benzotellurol-2-yl]oxy]tellurium(VI).

0002-7863/88/1510-6541$01.50/0

Table I. Crystal Data and Details of Crystal Structure Determination of $Te[OTe(C_8H_8)(S_2P(OEt)_2)]_6$

formula	$C_{72}H_{108}O_{18}P_6S_{12}Te_7$
M_r	2725.5
cryst syst	triclinic
space gp	$P\bar{1}$-C_i^1 (No. 2)
a, Å	14.287 (2)
b, Å	14.579 (2)
c, Å	14.652 (2)
α, deg	85.30 (1)
β, deg	84.36 (1)
γ, deg	60.20 (1)
V, Å^3	2633.5 (8)
Z	1
ρ_{calcd}, g cm^{-3}	1.72
ρ_{measd}, g cm^{-3}	1.72
cryst dimens, dist from centroid, mm	±(100), 0.140; ±(001), 0.133; (0$\bar{1}$0), 0.139; (120), 0.163; (1$\bar{1}\bar{1}$), 0.155
temp, K	295 (1)
radatn, Å	Mo Kα (graphite monochromator), λ = 0.71069
no. of intens control reflcns	3; measd every 3600 s; 10% decrease
F(000)	1330
μ, cm^{-1}	22.54; absorption corrcns applied with SHELX-76
transmissn factors	max 0.6077, min 0.5634
2θ limits	$2 \le 2\theta \le 44$
instrument	Enraf-Nonius CAD-4F diffractometer
no. of reflcns measd	7421
no. of unique reflcns	6456
R_{amal}	0.016
no. of reflcns used in refinement ($I \ge 2\sigma$)	4676
refinement	least squares; function minimized $\sum w\Delta^2$
R	0.051
R_w	0.056
hkl range	$-1 \le h \le 15$, $-15 \le k \le 15$, $-15 \le l \le 15$

nations of $Te(OTeF_5)_6$[3] and *trans*-$F_2Te(OTeF_5)_4$[6] together with solution NMR studies show that the geometry of the tellurium(VI) center is based on the octahedral oxygen bridge building principle. The central tellurium atom in $Te(OTeF_5)_6$ is bonded octahedrally to the six oxygen atoms of the $OTeF_5$ groups, each of which is also almost octahedral.

During the course of our investigations of the stereochemistry and bonding in hypervalent tellurium compounds in the solid state and in solution, several attempts were made to isolate crystals of $C_8H_8Te(Etdtp)_2$ (Etdtp = $S_2P(OEt)_2$) suitable for X-ray crystallography. In one such attempt a sample of $C_8H_8Te(Etdtp)_2$, in dichloromethane solution, was placed in a sealed vessel containing petroleum ether (40/60 °C). After a period of several months colorless crystals were obtained, which were first assumed to be $C_8H_8Te(Etdtp)_2$. Subsequent X-ray structural analysis, however, indicated that these were in fact crystals of the compound $Te^{VI}[OTe^{IV}(C_8H_8)(Etdtp)]_6$, which appears to be the first organotellurium mixed-valent complex. It also appears to be the first mixed-valent tellurium(VI)–tellurium(IV) complex prepared under such mild conditions. Subsequently, the following reaction scheme was developed so that $Te[OTe(C_8H_8)(Etdtp)]_6$ could be obtained more reliably from the following "one-pot" synthesis:

$$Te(OH)_6 + 6C_8H_8TeI_2 + 6KEtdtp + 6NEt_3 \rightarrow Te[OTe(C_8H_8)(Etdtp)]_6 + 6Et_3N{\cdot}HI + 6KI$$

We now report the synthesis and X-ray structure determination of $Te[OTe(C_8H_8)(Etdtp)]_6$ together with solution ^{13}C, ^{31}P, and

(1) Deakin University.
(2) University of Melbourne.
(3) Lentz, D.; Pritzkow, H.; Seppelt, K. *Inorg. Chem.* **1978**, *17*, 1926.
(4) Collins, M. J.; Schrobilgen, G. J. *Inorg. Chem.* **1985**, *24*, 2608.
(5) Birchall, T.; Myers, R. D.; De Waard, H.; Schrobilgen, G. J. *Inorg. Chem.* **1982**, *21*, 1068.
(6) Pritzkow, H.; Seppelt, K. *Inorg. Chem.* **1977**, *16*, 2685.

Table II. Final Fractional Atomic Coordinates for $Te[OTe(C_8H_8)(S_2P(OEt)_2)]_6$ (ESD's Given in Parentheses)[a]

	x	y	z
Te(1)	0.00000	0.00000	0.00000
Te(2)	0.11314 (6)	−0.05459 (6)	0.20995 (5)
O(2,1)	−0.0178 (5)	0.0092 (5)	0.1314 (4)
C(2,1)	0.1014 (10)	0.0965 (10)	0.2120 (8)
C(2,2)	0.0217 (10)	0.1515 (10)	0.2938 (8)
C(2,3)	0.0036 (13)	0.2551 (12)	0.3127 (11)
C(2,4)	−0.0668 (15)	0.3008 (14)	0.3901 (12)
C(2,5)	−0.117 (2)	0.253 (2)	0.4449 (13)
C(2,6)	−0.0956 (12)	0.1505 (12)	0.4242 (10)
C(2,7)	−0.0251 (9)	0.1021 (9)	0.3457 (8)
C(2,8)	−0.0067 (10)	−0.0051 (9)	0.3224 (8)
S(2,1)	0.2547 (3)	−0.1157 (3)	0.3406 (2)
S(2,2)	0.3769 (4)	−0.1244 (4)	0.1315 (3)
P(2,1)	0.3836 (4)	−0.1898 (4)	0.2527 (4)
O(2,2)	0.3971 (12)	−0.3093 (13)	0.2275 (11)
C(2,9)	0.414 (2)	−0.390 (2)	0.298 (2)
C(2,10)	0.430 (2)	−0.476 (2)	0.253 (2)
O(2,3A)	0.486 (2)	−0.243 (2)	0.296 (2)
O(2,3B)	0.470 (2)	−0.163 (2)	0.322 (2)
C(2,11A)	0.559 (3)	−0.210 (5)	0.293 (3)
C(2,11B)	0.560 (4)	−0.163 (6)	0.284 (4)
C(2,12A)	0.632 (3)	−0.264 (4)	0.370 (3)
C(2,12B)	0.584 (5)	−0.162 (6)	0.382 (4)
Te(3)	−0.26830 (6)	0.17567 (6)	0.05774 (5)
O(3,1)	−0.1241 (5)	0.1375 (5)	−0.0137 (4)
C(3,1)	−0.2278 (10)	0.2453 (10)	0.1584 (8)
C(3,2)	−0.2686 (11)	0.3589 (10)	0.1251 (9)
C(3,3)	−0.2578 (14)	0.4270 (14)	0.1822 (12)
C(3,4)	−0.299 (2)	0.539 (2)	0.1523 (15)
C(3,5)	−0.347 (2)	0.569 (2)	0.0687 (15)
C(3,6)	−0.3593 (13)	0.5035 (13)	0.0155 (11)
C(3,7)	−0.3148 (10)	0.3951 (10)	0.0434 (8)
C(3,8)	−0.3243 (10)	0.3201 (9)	−0.0176 (8)
S(3,1)	−0.4691 (3)	0.2643 (4)	0.1387 (3)
S(3,2)	−0.2997 (4)	0.0404 (4)	0.2484 (3)
P(3,1)	−0.4338 (4)	0.1769 (4)	0.2536 (3)
O(3,2A)	−0.4410 (13)	0.2544 (13)	0.3310 (12)
O(3,2B)	−0.444 (2)	0.093 (2)	0.174 (2)
C(3,9A)	−0.404 (2)	0.232 (3)	0.421 (2)
C(3,9B)	−0.439 (4)	0.021 (4)	0.095 (4)
C(3,10A)	−0.419 (3)	0.320 (3)	0.456 (2)
C(3,10B)	−0.514 (5)	0.034 (4)	0.035 (4)
O(3,3)	−0.5413 (15)	0.1680 (15)	0.2911 (13)
C(3,11)	−0.550 (2)	0.101 (2)	0.241 (2)
C(3,12)	−0.667 (3)	0.133 (3)	0.301 (3)
Te(4)	0.08914 (7)	0.16325 (6)	−0.11263 (5)
O(4,1)	0.0914 (6)	0.0620 (5)	−0.0063 (4)
C(4,1)	0.2217 (12)	0.1555 (12)	−0.0499 (10)
C(4,2)	0.1697 (13)	0.2511 (12)	0.0104 (10)
C(4,3)	0.255 (2)	0.263 (2)	0.0521 (14)
C(4,4)	0.197 (2)	0.354 (2)	0.110 (2)
C(4,5)	0.103 (2)	0.4142 (15)	0.1260 (12)
C(4,6)	0.0190 (15)	0.4003 (14)	0.0826 (12)
C(4,7)	0.0659 (11)	0.3108 (11)	0.0222 (9)
C(4,8)	−0.0150 (10)	0.2954 (10)	−0.0268 (9)
S(4,1)	0.1065 (4)	0.3076 (4)	−0.2327 (3)
S(4,2)	−0.1170 (4)	0.2975 (3)	−0.2547 (3)
P(4,1)	−0.0012 (4)	0.3145 (4)	−0.3139 (3)
O(4,2A)	0.0560 (13)	0.2049 (12)	−0.3796 (10)
O(4,2B)	0.068 (3)	0.284 (3)	−0.404 (2)
C(4,9A)	0.146 (3)	0.180 (3)	−0.435 (3)
C(4,9B)	0.154 (6)	0.185 (5)	−0.402 (5)
C(4,10A)	0.186 (2)	0.082 (2)	−0.481 (2)
C(4,10B)	0.206 (5)	0.129 (6)	−0.490 (4)
O(4,3A)	−0.029 (3)	0.442 (3)	−0.355 (2)
O(4,3B)	−0.034 (2)	0.394 (2)	−0.397 (2)
C(4,11A)	−0.132 (3)	0.488 (4)	−0.380 (4)
C(4,11B)	−0.096 (6)	0.500 (5)	−0.360 (4)
C(4,12A)	−0.211 (5)	0.603 (4)	−0.392 (5)
C(4,12B)	−0.154 (4)	0.554 (4)	−0.445 (4)

[a] Atoms of the ethoxide moieties designated A and B are disordered over the two sites with the following site occupation factors. O(2,3), C(2,11), C(2,12): site A, 0.45 (3); site B, 0.55 (3). O(3,2), C(3,9), C(3,10): site A, 0.77 (1); site B, 0.23 (1). O(4,2), C(4,9), C(4,10): site A, 0.64 (3); site B, 0.36 (3). O(4,3), C(4,11), C(4,12): site A, 0.55 (4); site B, 0.45 (4).

^{125}Te NMR data as well as CPMAS ^{13}C data for the solid state. The homologous complex Te[OTe(C_8H_8)(^{i}Prdtp)]$_6$ has also been prepared and characterized in solution by NMR spectroscopy.

Experimental Section

Materials. All solvents and reagents used were AR grade or better.

Preparation of Te[OTe(C_8H_8)(Rdtp)]$_6$ (R = Et, ^{i}Pr). The colorless crystal of Te[OTe(C_8H_8)(Etdtp)]$_6$ used for the X-ray diffraction data collection was isolated from a dichloromethane–petroleum ether (40/60 °C) solution of $C_8H_8Te(Etdtp)_2$. This crystal was one of apparently many products, as judged by the morphology of the crystals, adhering to the glass walls of the vessel.

Te[OTe(C_8H_8)(Etdtp)]$_6$ can be synthesized from a one-pot synthesis with orthotelluric acid:

$$Te(OH)_6 + 6C_8H_8TeI_2 + 6KEtdtp + 6NEt_3 \rightarrow Te[OTe(C_8H_8)(Etdtp)]_6 + 6Et_3N{\cdot}HI + 6KI$$

Orthotelluric acid,[7] 0.23 g (1 mmol), was dissolved in 50 cm^3 of dimethylformamide. The solution was warmed slightly to help dissolution. To this was added 2.92 g (6 mmol) $C_8H_8TeI_2$[8] and (6 mmol) KRdtp (R = Et, ^{i}Pr). The solution was stirred for several minutes, after which triethylamine, 0.9 cm^3 (6 mmol), was added dropwise. Stirring was continued for 2 h, and the solution was then poured into 200 cm^3 of distilled water, which causes the precipitation of a white solid. The precipitate was collected by filtration, washed with water, and air dried. The complex, Te[OTe(C_8H_8)(Etdtp)]$_6$, was obtained as a white powder with a yield of 76%. The yield of Te[OTe(C_8H_8)(^{i}Prdtp)]$_6$, also obtained as a white powder, was 82%. Both complexes decompose without melting; they begin to darken at 135 °C, eventually turning black at 150 °C. Crystals of both complexes can be obtained from slow vapor diffusion of petrol into a solution of Te[OTe(C_8H_8)(Rdtp)]$_6$ in dichloromethane.

Elemental Analyses. Analyses were performed by the Australian Microanalytical Service (Amdel). Anal. Calcd for Te[OTe(C_8H_8)(Etdtp)]$_6$: C, 31.73; H, 3.99. Found: C, 31.4; H, 3.6. Anal. Calcd for Te[OTe(C_8H_8)(^{i}Prdtp)]$_6$: C, 34.86; H, 4.60. Found: C, 34.5; H, 4.4.

Instrumentation. NMR spectra were routinely recorded on a JEOL FX 100 spectrometer with broad-band proton decoupling. A JEOL NM 5471 controller was used for temperature control; the temperatures in the probe were measured with a calibrated platinum resistance thermometer. ^{31}P spectra were recorded at 40.26 MHz and ^{13}C spectra at 25.00 MHz with external 85% H_3PO_4 and TMS, respectively, to reference chemical shifts. ^{125}Te spectra were recorded at 31.4 MHz usually on a 20-kHz spectral window; pulse width was 22 μs and the pulse delay 50 ms. Spectra were recorded in the presence of Cr(acac)$_3$ to reduce relaxation times. ^{125}Te chemical shifts were referenced against external 0.7 M K_2TeO_3 in water. Several spectra were also recorded at higher field with either a JEOL GX 270-MHz or a JEOL GX 400-MHz spectrometer. The solid-state CPMAS $^{13}C\{^1H\}$ spectra were recorded on a Bruker 300-MHz instrument at the University of Adelaide.

Crystal Structure Determination of Te[OTe(C_8H_8)(Etdtp)]$_6$: Crystallographic Data. Oscillation and Weissenberg photographs showed no symmetry other than that required by Friedel's law, indicating that the crystals were triclinic. The photographs also showed that the crystals possessed substantial disorder, especially at high Bragg angles, and attempts to find crystals that showed little disorder were unsuccessful. A crystal was mounted on a CAD-4F four-circle, single-crystal automatic diffractometer. Accurate cell dimensions were obtained from the setting angles of 25 reflections measured with Mo Kα (graphite monochromatized) radiation (λ = 0.71069 Å), by a least-squares procedure. The similarity of the axis lengths and the fact that one angle was close to 60° were noted. Further investigation, using the cell-reduction programs TRACERA[9] and the CAD-4F routine TRANS,[10] indicated that no cell of higher symmetry could be found.

Data Collection and Reduction. The crystal data appear in Table I. Integrated intensity data were collected by the ω–2θ scan method to a maximum Bragg angle of 22°; no reflection could be observed above a θ value of 22°. There was a 10% decrease in intensity of the intensity control reflections during the data collection, and the data were corrected in accordance with this variation, together with Lorentz, polarization, and absorption effects, but not for extinction. Absorption corrections were numerically evaluated by Gaussian integration to a precision of 0.5%.[11a,12]

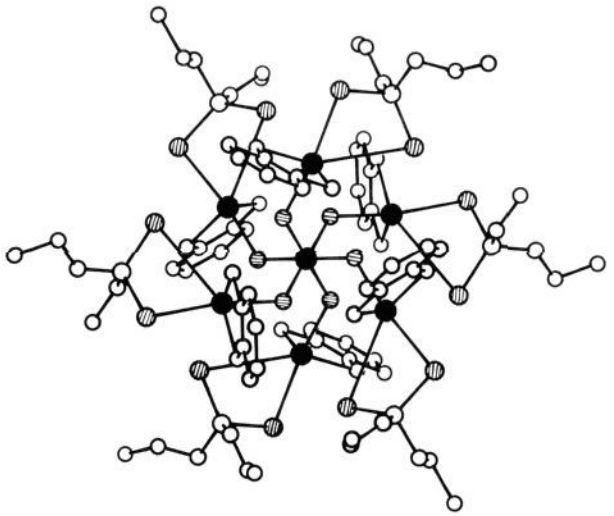

Figure 1. ORTEP diagram showing the overall view of the molecule Te[OTe(C_8H_8)(Etdtp)]$_6$. Tellurium atoms are represented by filled circles ●, sulfur atoms, by vertically hatched circles ⊘, and oxygen atoms bonded to tellurium, by horizontally hatched circles ⊖. For clarity only one set of sites for each of the disordered ethoxy groups has been included.

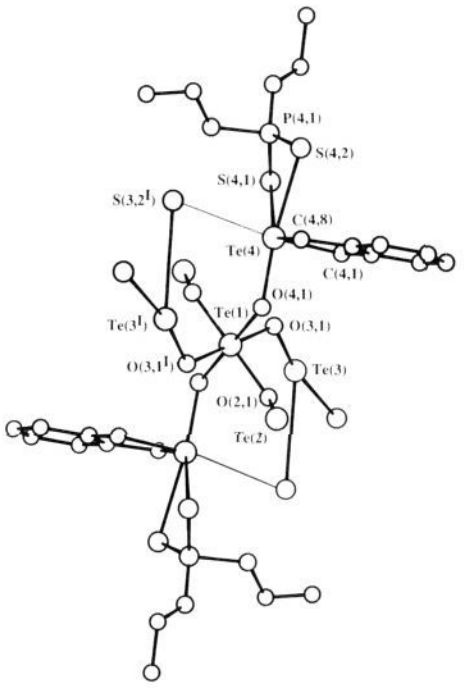

Figure 2. View of the tellurium(IV) and tellurium(VI) portions of the molecule Te[OTe(C_8H_8)(Etdtp)]$_6$ showing the numbering scheme employed. Substituents on all except Te(4) are omitted for clarity.

Other details concerning the data collection are given in Table I.

Structure Determination. The positions of three tellurium atoms, all in general positions, were located from a three-dimensional Patterson synthesis. From the subsequent difference map the positions of all other atoms were located, except for those belonging to the ethoxy groups. The structure was refined by a full-matrix least-squares refinement procedure; the function minimized is given in Table I. Anisotropic temperature factors were assigned to the tellurium, sulfur, and oxygen atoms, and isotropic thermal parameters were assigned to the carbon atoms of the C_8H_8 group. The difference map at this stage showed a number of very broad peaks, of about 2–4 e Å^{-3}, due to the atoms of the ethoxy groups

(7) Timofeev, S. A. *Zh. Obshch. Khim.* **1983**, *53*, 2237.
(8) Ziolo, R. F.; Günther, W. H. H. *J. Organomet. Chem.* **1978**, *146*, 245.
(9) Lawton, S. L.; Jacobson, R. A. *The Reduced Cell and Its Crystallographic Applications*; Iowa State University: Ames, IA, 1965.
(10) Enraf-Nonius, Program System for CAD-4F Diffractometer, Delft, The Netherlands, 1980.
(11) Ibers, J. A., Hamilton, W. C., Eds. *International Tables for X-ray Crystallography*; Kynoch: Birmingham, U.K., 1974; (a) Vol. IV, p 55; (b) Vol. IV, p 99; (c) Vol. IV, p 149.
(12) Sheldrick, G. M. *SHELX-76, Program for Crystal Structure Determination*; University of Cambridge: Cambridge, U.K., 1976.

Table III. Selected Bond Lengths (Å) for $Te[OTe(C_8H_8)(Etdtp)]_6$

atoms	separation $n = 2$	$n = 3$	$n = 4$
Te(1)···Te(n)	3.4651 (8)	3.4537 (9)	3.4592 (9)
Te(1)···O(n,1)	1.924 (6)	1.917 (7)	1.915 (9)
Te(n)–O(n,1)	2.051 (7)	2.045 (8)	2.048 (6)
Te(n)–C(n,1)	2.127 (13)	2.130 (14)	2.165 (13)
Te(n)–C(n,8)	2.140 (13)	2.100 (12)	2.13 (2)
Te(n)–S(n,1)	2.691 (4)	2.684 (5)	2.722 (5)
Te(n)–S(n,2)	3.477 (6)	3.410 (5)	3.413 (5)
C(n,1)···C(n,8)	2.93 (2)	2.91 (2)	2.96 (2)
S(n,1)···S(n,2)	3.353 (6)	3.339 (7)	3.317 (9)
Te(n)···P(n,1)	3.451 (6)	3.530 (5)	3.475 (5)
S(n,1)–P(n,1)	2.000 (7)	1.972 (7)	1.995 (8)
S(n,2)–P(n,1)	1.933 (7)	1.960 (8)	1.908 (8)
Te(2)–S(4,2)[a]	3.522 (5)		
Te(3)–S(2,2)[a]	3.605 (5)		
Te(4)–S(3,2)[a]	3.569 (5)		

[a] $-x, -y, -z$.

Table IV. Selected Bond Angles (deg) for $Te[OTe(C_8H_8)(Etdtp)]_6$

atoms	angles	atoms	angles
O(2,1)–Te(1)–O(3,1)	90.8 (3)	O(2,1)–Te(1)–O(4,1)	90.4 (3)
O(2,1)–Te(1)–O(3,1)[a]	89.2 (3)	O(2,1)–Te(1)–O(4,1)[a]	89.6 (3)
O(3,1)–Te(1)–O(4,1)	90.3 (3)	O(3,1)–Te(1)–O(4,1)[a]	89.7 (3)

atoms	angles $n = 2$	$n = 3$	$n = 4$
Te(1)–O(n,1)–Te(n)	121.3 (4)	121.3 (3)	121.6 (4)
O(n,1)–Te(n)–C(n,1)	89.9 (4)	89.4 (4)	89.2 (4)
O(n,1)–Te(n)–C(n,8)	83.9 (4)	84.1 (4)	84.3 (5)
O(n,1)–Te(n)–S(n,1)	168.2 (2)	168.8 (2)	169.1 (3)
O(n,1)–Te(n)–S(n,2)	126.0 (2)	124.9 (2)	124.8 (3)
C(n,1)–Te(n)–C(n,8)	86.7 (5)	87.0 (5)	86.9 (6)
C(n,1)–Te(n)–S(n,1)	86.4 (4)	87.7 (4)	86.3 (4)
C(n,1)–Te(n)–S(n,2)	81.3 (4)	80.9 (4)	81.6 (4)
C(n,8)–Te(n)–S(n,1)	84.7 (4)	84.9 (4)	85.5 (4)
C(n,8)–Te(n)–S(n,2)	147.4 (4)	148.0 (4)	148.2 (4)
S(n,1)–Te(n)–S(n,2)	64.40 (12)	65.19 (14)	64.3 (2)
Te(n)–C(n,1)–C(n,2)	105.5 (9)	105.4 (9)	102.7 (9)
Te(n)–C(n,8)–C(n,7)	105.2 (9)	106.0 (8)	104.2 (1.2)
Te(n)–S(n,1)–P(n,1)	93.6 (2)	97.4 (3)	93.6 (3)
Te(n)–S(n,2)–P(n,1)	73.1 (3)	77.0 (2)	75.7 (2)
S(n,1)–P(n,1)–S(n,2)	116.9 (3)	116.2 (3)	116.3 (3)
Te(n)–S(n,2)–Te(3)[a]	75.85 (13)		
Te(3)–S(3,2)–Te(4)[a]	76.78 (10)		
Te(4)–S(4,2)–Te(2)[a]	77.0 (8)		
P(n,1)–S(n,2)–Te(3)[a]	123.5 (3)		
P(3,1)–S(3,2)–Te(4)[a]	148.5 (2)		
P(4,1)–S(4,2)–Te(n)[a]	125.4 (2)		

[a] $-x, -y, -z$.

of the dithiophosphate ligands, which indicated that these atoms were disordered. It was possible to account for the disorder of four of the ethoxy groups by assuming each atom to be distributed over two positions, with each group of atoms being assigned a refinable site-occupation factor. For the other two ethoxy groups this was not possible. Refinement was continued with isotropic thermal parameters assigned to these atoms. During the refinement some of these atoms were constrained to having O–C and C–C bond lengths of 1.35 and 1.50 Å, respectively; no other constraints were applied. The difference map at this stage showed peaks of about 0.5–0.8 e Å^{-3} close to the carbon atoms of the C_8H_8 groups, suggesting either anisotropic thermal motion or disorder. An attempted refinement with these atoms being assigned anisotropic thermal parameters resulted in extremely high thermal parameters for some of these atoms, indicating that they too were somewhat disordered. As it was not possible to account for the disorder, refinement was continued with these atoms having isotropic thermal parameters. No hydrogen atoms were located from the difference maps, and none were included in the model. The final difference map showed peaks whose maximum heights were 1.1 e Å^{-3} around the ethoxy ligands. All other peaks in the difference map were less than 0.8 e Å^{-3}. The weighting scheme employed was of the form $w = k/(\sigma^2(F) + gF^2)$ where the parameters k and g were varied during the course of refinement. An analysis of variance showed that an appropriate weighting scheme had been applied. Final values for R, R_w, k, and g are 0.051, 0.056, 2.48, and 0.00050. Final fractional atomic coordinates are given in Table II.

Table V. ^{13}C Data for $Te[OTe(C_8H_8)(Etdtp)]_6$ (1), $C_8H_8Te(Etdtp)_2$ (2), and $Te[OTe(C_8H_8)(^iPrdtp)]_6$ (3)

compd	carbon atom[a] 1	2	3	4	5	6
1 (rt in tce soln)	47.6 br	139.9	130.5	127.8	63.3[b]	16.5[c]
	55.0 br	141.1	131.7			
1 (solid state)	43.3, 51.9	124.0–139.1			59.3	13.8
	46.8, 54.9				60.7	15.3
2 (solid state)	40.6	136.8	125.0	128.4	61.2	13.6
	54.6	138.5	126.3			14.6
3 (rt in dcm soln)	47.2	140.0	130.0	127.5 br	72.2[b]	24.1
	55.5	141.4	131.6			
3 (−55 °C in $CDCl_3$ soln)	46.6		130.1	127.1	71.2	23.8
	54.9		131.2	127.2	71.9	24.4

[a] Assignments given in Figure 3. [b] $^2J_{C-P} = 6$ Hz. [c] $^3J_{C-P} = 10$ Hz.

Calculations were carried out with the programs SHELX-76,[12] ORTEP,[13] and DISTAN[14] on a VAX 11/780 computer at the University Computer Services. Scattering curves for atomic H, C, O, P, and S were those collected by Sheldrick,[12] while that of Te was taken from ref 11b, the value being corrected for the real and imaginary dispersion terms.[11c]

Description of the Structure of $Te[OTe(C_8H_8)(Etdtp)]_6$. An ORTEP diagram of the molecule is given in Figure 1 with the atomic numbering scheme given in Figure 2. Important bond distances and angles are listed in Tables III and IV, respectively. The structure consists of discrete $Te[OTe(C_8H_8)(Etdtp)]_6$ molecules. The central tellurium(VI) atom, located at a center of symmetry, is bonded octahedrally to six oxygen atoms with a maximum deviation of 0.8° from ideal angles, which in turn bond to two sets of three crystallographically unique tellurium(IV) atoms. Apart from the terminal ethyl groups, the structure has a symmetry that is close to $\bar{3}$. The mean tellurium(VI)–oxygen distance is 1.919 (7) Å as compared with 1.902 Å found in the structure of $Te(OTeF_5)_6$.[3] The average Te(VI)–O–Te(IV) angle in $Te[OTe(C_8H_8)(Etdtp)]_6$ is 121.4 (4)°, compared with 139.0° found in $Te(OTeF_5)_6$.[3] The Te–O–Te angles found in $Te[OTe(C_8H_8)(Etdtp)]_6$ are substantially greater than the ideal value expected for this moiety. Oxygen-bridging angles greater than 109° are indicative of a π interaction between the p orbitals of the bridging oxygens and the d orbitals of the tellurium atom.[3] The tellurium(IV)–oxygen distance in $Te[OTe(C_8H_8)(Etdtp)]_6$ [2.048 (7) Å] is comparable with other Te(IV)–O distances. This is longer than the corresponding tellurium(VI)–oxygen distance (Te(VI)–O, 1.919 Å), in accord with a lower oxidation state of the metal.

The *o*-xylene-α,α'-diyl chelates (i.e. C_8H_8) are approximately perpendicular to the tellurium(IV)–oxygen bonds and are arranged such that (i.e. viewing the molecules as in Figure 1) three chelates are directed into the page and three out of the page. This propeller-like arrangement minimizes ring repulsions and is likely to provide a certain amount of rigidity to the structure in solution. Each diethyldithiophosphate ligand is anisobidentically chelated to a tellurium(IV) center. The mean tellurium–sulfur distances are 2.699 (5) and 3.433 (5) Å. The sulfur closest to each tellurium(IV) is approximately trans to the oxygen atom (mean S–Te–O angle 168.7°). The sulfur of the longer Te–S bond also forms a secondary interaction with an adjacent tellurium(IV) center (average distance 3.565 (5) Å) within the same molecule. An appreciable number of solid-state structures contain secondary bonds,[15] which are interactions longer than the sum of the respective covalent radii but shorter than the sum of their van der Waals radii. Secondary bonds increase the overall effective coordination of the central atom and are often in the region of space about the central atom that is thought to be occupied by a lone electron pair. One particularly relevant example is observed in $C_8H_8Te(Etdtp)_2$[16] where the secondary bonding is intermolecular in nature (Te–S 3.729 Å), leading to formation of a zigzag polymeric chain structure throughout the crystal.

The stereochemistry about the tellurium(IV) centers in $Te[OTe(C_8H_8)(Etdtp)]_6$ conforms to a distorted seven-coordinate 1:2:2:2 geometry,[17] with the seventh position occupied by a stereochemically active lone pair of electrons. The lone pair of electrons residing on the tellurium is opposite to, and in the plane of, the C_8H_8 chelate. Each lone pair is

(13) Johnson, C. K. *ORTEP*; Report ORNL-3794; Oak Ridge National Laboratory: Oak Ridge, TN, 1965.
(14) Kelly, B. P.; O'Day, B. P.; Pannan, C. D., University of Melbourne, 1974.
(15) Alcock, N. W. *Adv. Inorg. Chem. Radiochem.* **1972**, *15*, 1.
(16) Dakternieks, D.; Di Giacomo, R.; Gable, R. W.; Hoskins, B. F. *J. Am. Chem. Soc.*, in press.
(17) Claxton, T. A.; Benson, G. C. *Can. J. Chem.* **1966**, *44*, 157.

directed toward that region of space that lies between the two longer tellurium–sulfur interactions.

NMR Study of Te[OTe(C_8H_8)(Etdtp)]$_6$ and C_8H_8Te(Etdtp)$_2$. The ^{125}Te spectrum of a dichloromethane solution of Te[OTe(C_8H_8)(Etdtp)]$_6$ at room temperature contains a doublet resonance at $\delta(^{125}Te)$ −670 ($^2J_{Te-P}$ = 103 Hz) ppm and a singlet at −1016 ppm, which have integrated intensities of 6:1. Lowering the temperature to −100 °C causes no change to the ^{125}Te spectrum, apart from improving the resolution. The $^{31}P\{^1H\}$ spectrum at −100 °C contains only one resonance, $\delta(^{31}P)$ 100.5 ppm, with ^{125}Te satellites ($^2J_{P-Te}$ = 107 Hz). Thus, the doublet tellurium resonance is assigned to six equivalent tellurium(IV) centers, each of which couples to the phosphorus atom of one of the six equivalent dithiophosphate ligands. A ^{125}Te spectrum obtained by a higher field spectrometer (i.e. JEOL GX, 270 MHz) verified that the ^{125}Te doublet centered at −670 ppm is indeed due to phosphorus–tellurium coupling. No evidence was observed for tellurium(IV)–tellurium(VI) coupling through the oxygen atom. Observation of two-bond tellurium–phosphorus coupling at room temperature was unexpected since previously J_{P-Te} was observed only at low temperature when monodentate–bidentate exchange of the dithiophosphate ligand is slow on the NMR time scale,[16] the magnitude of the coupling being approximately 30 Hz in those cases.

The $^{13}C\{^1H\}$ spectrum of Te[OTe(C_8H_8)(Etdtp)]$_6$ in tetrachloroethane (tce) recorded at room temperature with a 100-MHz spectrometer shows two resonances for the ethyl carbon atoms (Table V) of the dithiophosphate ligands, indicative of six equivalent dithiophosphate ligands. The benzylic carbon atoms adjacent to the tellurium atom give two broad but well-separated ^{13}C resonances and five resonances are observed for the aromatic carbons. Lowering the temperature leads to line broadening and a loss of resolution. There was no significant improvement in resolution when the ^{13}C spectrum was obtained in $CDCl_3$ solvent at higher field (i.e. a JEOL GX, 400 MHz).

The solid-state CPMAS $^{13}C\{^1H\}$ spectrum, recorded on a Bruker 300-MHz instrument, is more complex. The methyl carbon atoms of the dithiophosphate ligand give two well-separated resonances. The methylene carbon atoms give two resonances, and it could not be determined whether the multiplicity of these two resonances arises from two-bond coupling to ^{31}P. Four resonances are observed for the methylene carbon atoms adjacent to the tellurium atom (Table V) and the aromatic carbon atoms give rise to a number of resonances in the range 124.0–139.1 ppm, but none could be assigned. The complexity of the ^{13}C spectrum may result from the fact that the molecule contains two sets of three crystallographically different tellurium(IV) centers.

The solid-state ^{13}C spectrum of the "parent" compound, C_8H_8Te(Etdtp)$_2$, is similar to the ^{13}C spectrum of Te[OTe(C_8H_8)(Etdtp)]$_6$ in solution. The methyl carbon atoms of the dithiophosphate ligand in C_8H_8Te(Etdtp)$_2$ give two resonances (Table V). The dithiophosphate methylene carbon atoms give rise to a single resonance, whereas the methylene carbon atoms adjacent to the tellurium atom give two well-separated resonances. The aromatic carbon atoms corresponding to positions 4 and 4′ (Figure 3) give a single resonance whereas the individual resonances are observed for the carbon atoms at positions 2 and 2′ and positions 3 and 3′. If the geometry of the molecule is static on the NMR time scale, a total of eight resonances should be observed for carbon atoms of the planar *o*-xylene-α,α'-diyl (i.e. C_8H_8) ligand in Figure 3 (i.e. four sets of doublets). The separation of each doublet should decrease with increasing distance from the tellurium atom, which is the center of the asymmetry. The fact that only seven of the eight ^{13}C resonances are observed probably results from the inability of the spectrometer to resolve the two resonances for very similar carbon atoms in positions 4 and 4′.

The similarity of the solution ^{13}C spectrum for Te[OTe(C_8H_8)(Etdtp)]$_6$ with the solid-state ^{13}C spectrum of C_8H_8Te(Etdtp)$_2$ suggests that the former molecule remains rigid in solution. That could occur only if the bridging sulfur–tellurium interactions (Figure 2) remain intact in solution. Further supportive evidence for this dynamic rigidity lies in the observation of two-bond tellurium(IV)–phosphorus coupling, which implies that the dithiophosphate ligand remains chelated and does not undergo appreciable intramolecular monodentate–bidentate exchange, on the NMR time scale.

Solution NMR Study of Te[OTe(C_8H_8)(^{i}Prdtp)]$_6$. The ^{125}Te spectrum (Figure 4) of Te[OTe(C_8H_8)(^{i}Prdtp)]$_6$ in dichloromethane solution at room temperature comprises a doublet of doublets, $\delta(^{125}Te)$ −669 ppm, assigned to the six equivalent tellurium(IV) centers, and a singlet, $\delta(^{125}Te)$ −1006 ppm, assigned to the tellurium(VI) center. The integrated intensity ratio of the doublet of doublets to the singlet is 6:1. The larger coupling found in the tellurium(IV) resonance, 121 Hz, is assigned to two-bond phosphorus coupling (cf. $^2J_{Te-P}$ = 103 Hz for Te[OTe(C_8H_8)(Etdtp)]$_6$) whereas the origin of the smaller splitting, 23 Hz, is not immediately obvious.

The ^{13}C spectrum of a solution of Te[OTe(C_8H_8)(^{i}Prdtp)]$_6$ in tetrachloroethane at room temperature shows resonances of the expected

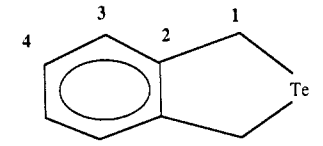

Figure 3. Atom labeling for the C_8H_8 portion of Te[OTe(C_8H_8)(Rdtp)]$_6$.

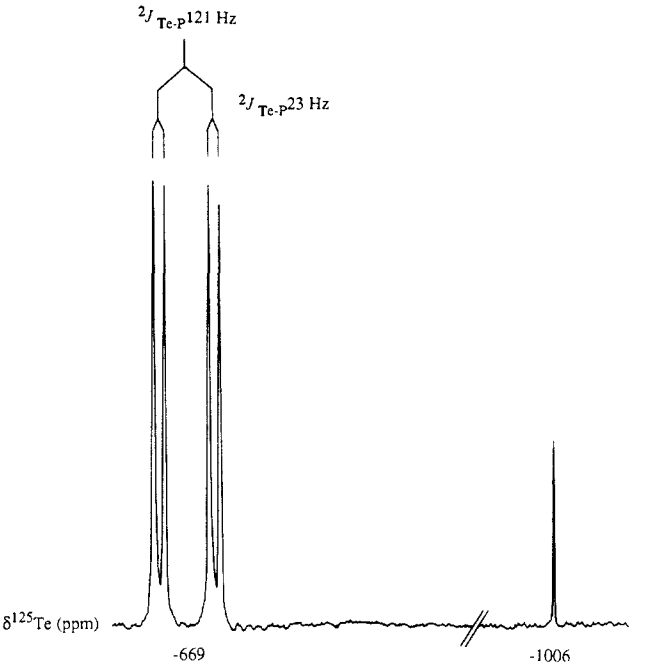

Figure 4. ^{125}Te spectrum of Te[OTe(C_8H_8)(^{i}Prdtp)]$_6$ in dcm solution at room temperature.

intensities for the methyl and methine carbon atoms in the dithiophosphate ligands (Table V). The methylene carbon atoms adjacent to the tellurium atom give two well-separated ^{13}C resonances as do the carbon atoms in positions 2 and 2′ and positions 3 and 3′ (Figure 3). The carbon atoms furthest away from the tellurium atom (i.e. positions 4 and 4′) give a single broad resonance [$\delta(^{13}C)$ 127.5 ppm]. The ^{13}C spectrum of a solution of Te[OTe(C_8H_8)(^{i}Prdtp)]$_6$ in $CDCl_3$ recorded on a higher field instrument (i.e. JEOL GX, 270 MHz) at −55 °C shows all eight ^{13}C resonances for the *o*-xylene-α,α'-diyl ligand with the resonances for the two carbon atoms in positions 4 and 4′ now resolved (Table V) as are the methine carbon resonances. The dithiophosphate methyl carbon atoms are also resolved into two broad ^{13}C resonances.

The $^{31}P\{^1H\}$ spectrum of Te[OTe(C_8H_8)(^{i}Prdtp)]$_6$ at room temperature consists of a single sharp resonance [$\delta(^{31}P)$ 96.4 ppm] with apparently two sets of satellites [$^2J_{P-Te}$ = 122 Hz; $^2J_{P-Te}$ = 23 Hz]. The $^{31}P\{^1H\}$ spectrum obtained with a higher field spectrometer (JEOL GX, 270 MHz) gives a sharp resonance ($w_{1/2}$ = 1 Hz) at identical chemical shift position to that recorded on the lower field instrument. The narrow width of the ^{31}P resonance confirms that it is a singlet and indicates that the two different phosphorus atoms almost certainly do not couple to each other.

The multiplicity of the tellurium(IV) resonance can now be rationalized by examination of the solid-state structure of Te[OTe(C_8H_8)(Etdtp)]$_6$, described above, in which the dithiophosphate ligand is anisobidentically chelated to the tellurium(IV) atom by a short and a long tellurium–sulfur bond (Figure 2). Furthermore, the sulfur involved in the longer tellurium–sulfur bond also interacts with an adjacent tellurium(IV) atom in the same molecule. If the structure adopted in solution is similar to that in solid-state structure, it might be expected that each tellurium(IV) atom would couple to the phosphorus atom of the dithiophosphate ligand to which it was strongly bonded ($^2J_{Te-P}$ = 121 Hz) as well as coupling to a second phosphorus atom from the adjacent dithiophosphate ligand via the bridging sulfur atom. Thus, the doublet of doublets observed in the ^{125}Te spectrum of Te[OTe(C_8H_8)(^{i}Prdtp)]$_6$ is assigned on this basis. Observation of both tellurium–phosphorus couplings in Te[OTe(C_8H_8)(^{i}Prdtp)]$_6$ implies that this compound is more rigid in solution than is Te[OTe(C_8H_8)(Etdtp)]$_6$, presumably due to static gearing of the isopropyl group.[18]

(18) Reference 16 and references therein.

The observation of tellurium–phosphorus coupling of 107 and 121 Hz in the complexes $Te[OTe(C_8H_8)(Etdtp)]_6$ and $Te[OTe(C_8H_8)(^iPrdtp)]_6$, respectively, is unusual for main-group dithiophosphate complexes. Previously,[16] coupling ($^2J_{Te-P}$) was only observed for $C_8H_8Te(Rdtc)(Rdtp)$ (R = Et, ^{i}Pr) complexes where intramolecular monodentate–bidentate ligand-exchange processes are slow on the NMR time scale, usually at temperatures less than −20 °C. The observation of $^2J_{Te-P}$ coupling in $Te[OTe(C_8H_8)(Etdtp)]_6$ at room temperature indicates that the activation energy for monodentate–bidentate exchange is larger than those in the complexes discussed previously.[16] A high-temperature study of $Te[OTe(C_8H_8)(Etdtp)]_6$ in tetrachloroethane was undertaken to determine qualitatively the barrier to monodentate–bidentate exchange. The ^{125}Te spectrum at 40 °C is very similar to the room-temperature spectrum with the exception that the tellurium(IV) signals are broader. At 60 °C the tellurium(IV) signals broaden into an unsymmetrical singlet ($w_{1/2}$ = 120 Hz), and at 70 °C only two singlets are observed with the correct intensities of 6:1. Cooling the sample back to room temperature gives a ^{125}Te spectrum identical with the original spectrum at room temperature. The ^{125}Te spectrum at 90 °C shows that the sample begins to decompose as evidenced by the appearance of a new resonance at $\delta(^{125}Te)$ −991.4 ppm, which does not disappear when the sample is cooled to room temperature. ^{13}C and ^{31}P spectra also confirm that the sample decomposes at 90 °C.

A similar experiment was conducted on the complex $Te[OTe(C_8H_8)(^iPrdtp)]_6$. At 60 °C in tetrachloroethane the tellurium(IV) resonances are not yet coalesced, but at 80 °C the tellurium(IV) resonances collapse into a broad singlet. The intermediate situation, with only the larger coupling ($^2J_{Te-P}$ = 121 Hz) to the tellurium atom, was not observed. Returning the temperature to 30 °C again results in observation of the doublet of doublets. The fact that the smaller coupling ($^2J_{Te-P}$ = 23 Hz) does not disappear before the larger coupling ($^2J_{Te-P}$ = 121 Hz) implies that disruption of the intramolecular interaction via the bridging sulfur occurs at about the same temperature at which intramolecular monodentate–bidentate exchange of the dithiophosphate ligand becomes rapid on the NMR time scale. The above data support the premise, surmised from the solid-state structure, that the inherent rigidity caused by the bonding and arrangement of the ligands in the molecule persists in solution at room temperature.

Conclusions

Mixed-valent tellurium(IV)–tellurium(VI) compounds can be synthesized easily under surprisingly mild conditions. Variable-temperature multinuclear magnetic resonance techniques have proved to be extremely valuable in determining the structures of these complexes in solution. The solution NMR data show that intramolecular monodentate–bidentate dithiolate exchange is slow on the NMR time scale. Furthermore, this appears to be the first example for which there is evidence that secondary bonds persist in solution. Consistent with NMR data, the solution geometries postulated appear to be similar to those observed in the solid state, thus suggesting that the stereochemical activity of the lone electron pair persists in solution.

Acknowledgment. We are grateful for a Commonwealth of Australia Postgraduate Research award to R.D. and the Australian Research Grants Scheme (ARGS) for financial assistance.

Registry No. 1, 115533-23-8; **2**, 115481-98-6; **3**, 115512-00-0; $Te(OH)_6$, 7803-68-1; $C_8H_8TeI_2$, 66149-48-2; KEtdtp, 3454-66-8; K^{i}Prdtp, 3419-34-9.

Supplementary Material Available: Tables S-I–S-III of anisotropic thermal parameters, isotropic C atom parameters, and bond lengths and angles for the C_6H_4 rings (3 pages); a listing of observed and calculated structure factor data (23 pages). Ordering information is given on any current masthead page.